0026-895X/08/7403-552–561$20.00
MOLECULAR PHARMACOLOGY
Copyright © 2008 The American Society for Pharmacology and Experimental Therapeutics
*Mol Pharmacol* 74:552–561, 2008

Vol. 74, No. 3
45054/3369286
*Printed in U.S.A.*

# Mutational Analysis of the Conserved Asp$^{2.50}$ and ERY Motif Reveals Signaling Bias of the Urotensin II Receptor

Christophe D. Proulx, Brian J. Holleran, Antony A. Boucard, Emanuel Escher, Gaétan Guillemette, and Richard Leduc

*Department of Pharmacology, Faculty of Medicine and Health Sciences, Université de Sherbrooke, Sherbrooke, Québec, Canada*

Received January 8, 2008; accepted May 22, 2008

## ABSTRACT

Class A (rhodopsin-like) G protein-coupled receptors possess conserved residues and motifs that are important for their specific activity. In the present study, we examined the role of residue Asp97$^{2.50}$ as well as residues Glu147$^{3.49}$, Arg148$^{3.50}$, and Tyr149$^{3.51}$ of the ERY motif on the functionality of the urotensin II receptor (UT). Mutations D97$^{2.50}$A, R148$^{3.50}$A, and R148$^{3.50}$H abolished the ability of UT to activate phospholipase C, whereas mutations E147$^{3.49}$A and Y149$^{3.51}$A reduced the ability to activate PLC by 50%. None of the mutants exhibited constitutive activity. However, R148$^{3.50}$A and R148$^{3.50}$H promoted ERK1/2 activation, which was abolished by 4-(3-chloroanilino)-6,7-dimethoxyquinazoline (AG1478), an inhibitor of epidermal growth factor receptor (EGFR) tyrosine kinase activity. Both these mutants were capable of directly activating EGFR, which confirmed that they activated the mitogen-activated protein kinase (MAPK) pathway by a $G\alpha_{q/11}$-independent transactivation of EGFR. The D97$^{2.50}$A, R148$^{3.50}$A, and R148$^{3.50}$H mutants did not readily internalize and did not promote translocation or colocalize with $\beta$-arrestin2-GFP. Finally, the agonist-induced internalization of the E147$^{3.49}$A mutant receptor was significantly increased compared with wild-type receptor. This study highlights the major contribution of the conserved Asp$^{2.50}$ residue to the functionality of the UT receptor. The Arg residue in the ERY motif of UT is an important structural element in signaling crossroads that determine whether $G\alpha_{q/11}$-dependent and -independent events can occur.

GPCRs, which make up the largest family of membrane proteins, are coded by more than 720 genes in the human genome (Wise et al., 2004). Of these, 280 belong to family A, which are classified by homology with rhodopsin (http://www.iupharbb.org/receptorList/results.php). Class A GPCRs respond to a wide array of ligands ranging from photons to large glycoproteins (Bockaert and Pin, 1999). More than 25% of clinically marketed drugs currently target class A GPCRs (Overington et al., 2006). In view of the broad range of biological functions and the great potential for pharmacological intervention, considerable interest has been generated in understanding the mechanisms by which GPCRs mediate their effects.

Overall homology among class A receptors is low and is restricted to a number of highly conserved key residues, suggesting that these residues play an essential role in the structural and/or functional integrity of these receptors. Most members of the rhodopsin-like family possess a conserved Asp residue (D$^{2.50}$) in transmembrane domain 2 (TMD2) and a Glu/Asp-Arg-Tyr (E/D$^{3.49}$-R$^{3.50}$-Y$^{3.51}$) motif at the junction of TMD3 and the second intracellular loop. Using different biochemical methods, several groups have demonstrated movements between TMD3 and TMD6 when receptors undergo activation (Gether et al., 1997). In rhodopsin, the basal inactive state is maintained by an ionic lock, where Arg$^{3.50}$ and Glu$^{3.49}$ form a network of ionic interactions with Glu$^{6.30}$ at the cytoplasmic end of TMD6 (Palczewski et al., 2000). Protonation of Glu$^{3.49}$

This work was supported by grants from the Canadian Institutes of Health Research (to E.E., G.G., and R.L.) and the Heart and Stroke Foundation (to R.L.). C.D.P. received a studentship from the Heart and Stroke Foundation of Canada. E.E. holds the J. C. Edwards Chair in Cardiovascular Research. R.L. is a Chercheur National of the Fonds de la Recherche en Santé du Québec. This work was part of the Ph.D. thesis of C.D.P.

Article, publication date, and citation information can be found at http://molpharm.aspetjournals.org.
doi:10.1124/mol.108.045054.

**ABBREVIATIONS:** GPCR, G protein-coupled receptor; TMD, transmembrane domain; UII, urotensin II; UT receptor, urotensin II receptor; MAPK, mitogen-activated protein kinase; DMEM, Dulbecco's modified Eagle's medium; AG1478, 4-(3-chloroanilino)-6,7-dimethoxyquinazoline; BIM, bisindolylmaleimide I; PCR, polymerase chain reaction; PBS, phosphate-buffered saline; IP, inositol phosphate; BSA, bovine serum albumin; ELISA, enzyme-linked immunosorbent assay; TBS, Tris-buffered saline; GFP, green fluorescent protein; D97$^{2.50}$A, myc-tagged urotensin II receptor with an Asp to Ala mutation at position 97; ANOVA, analysis of variance; ERK, extracellular signal-regulated kinase; PKC, protein kinase C; EGFR, epidermal growth factor receptor; V2R, vasopressin V2 receptor; HEK, human embryonic kidney.

in rhodopsin causes the pivoting movement between TMD3 and TMD6 and leads to receptor activation (Arnis et al., 1994). Mutations in Glu$^{3.49}$ and Glu$^{6.30}$ have been shown to promote constitutive activation of a number of GPCRs, suggesting that rhodopsin-like GPCRs may have similar activation mechanisms (Scheer et al., 1996; Ballesteros et al., 2001). However, replacement of Glu$^{3.49}$ does not always lead to constitutive activity (Chung et al., 2002; Feng and Song, 2003; Capra et al., 2004). In addition, the crystal structure of the $\beta$2-adrenergic receptor indicates that in the basal state, the distance between TMD3 and TMD6 is greater in this receptor than in rhodopsin, which would not allow interactions between specific residues in these domains to occur (Rosenbaum et al., 2007). Discrepancies in the functional effects revealed by mutational analyses of these residues in class A GPCRs and those deduced from the crystal structure of the $\beta$2-adrenergic receptor suggest alternative roles for the E/D$^{3.49}$ residue and the E/DRY motif in class A GPCRs. For example, based on simulations using the $\alpha_{1B}$-adrenergic receptor, Scheer et al. (1996) suggested that Arg$^{3.50}$ in the inactive state is constrained in a "polar pocket" formed by residues Asn$^{1.50}$, Asp$^{2.50}$, Asn$^{7.49}$, and Tyr$^{7.53}$.

Urotensin II (UII), a cyclic undecapeptide originally isolated from the caudal neurosecretory system of teleost fish, has since been identified in many classes of vertebrates, including humans (Douglas et al., 2004). Although it is clear that UII influences the physiological regulation of mammalian cardiovascular function, early studies led to conflicting reports of vasoactive responses, depending on the species or tissues studied, with UII acting both as a potent vasodilator (Stirrat et al., 2001) and a vasoconstrictor (Douglas et al., 2000). UII is the endogenous ligand for the G protein-coupled UT receptor (originally called GPR14) (Ames et al., 1999). The UT receptor belongs to the class A family of GPCRs. Upon UII binding, it functionally couples to G$\alpha_{q/11}$, thereby promoting phospholipase C activation (Saetrum Opgaard et al., 2000), $Ca^{2+}$ mobilization (Ames et al., 1999), and mitogen-activated protein kinase (MAPK) activation (Ziltener et al., 2002). UT is found in the central nervous system and is widely expressed in human tissues, including the left atrium and ventricle of the heart, smooth muscle cells in the coronary artery and aorta and endothelial cells in vascular beds (Douglas et al., 2004). Compelling evidence has implicated the urotensin system in the pathophysiology of hypertension, heart failure and of cardiac fibrosis and hypertrophy (Douglas et al., 2004).

Here, we investigate how substitution of the conserved residue Asp97$^{2.50}$ in TMD2 and Glu147$^{3.49}$, Arg148$^{3.50}$, and Tyr149$^{3.51}$ in the ERY motif affects binding, signaling, and internalization of the UT receptor. Our results demonstrate that Asp$^{2.50}$ plays a critical role in the activation of the UT receptor. Mutational analyses of the highly conserved Arg$^{3.50}$ reveal that this residue is important in G$\alpha_{q/11}$-protein-dependent UT signaling and reveals a G$\alpha_{q/11}$-protein-independent activation of the MAPK pathway.

## Materials and Methods

**Materials.** Bovine serum albumin and bacitracin were from Sigma-Aldrich (Oakville, ON, Canada). The cDNA encoding the rat UT receptor (GPR14) subcloned in the mammalian expression vector pcDNA3 was a generous gift from Dr. Brian O'Dowd (University of Toronto, Toronto, ON, Canada). Dulbecco's modified Eagle's medium (DMEM), fetal bovine serum, penicillin-streptomycin, and oligonucleotide primers were from Invitrogen (Carlsbad, CA); FuGENE-6, protease inhibitor cocktail, and mouse monoclonal anti-myc antibody were from Roche Molecular Biochemicals (Mannheim, Germany); and rabbit polyclonal antibodies directed against phosphorylated and active forms of p42/p44 MAPK were from New England Biolabs (Mississauga, ON, Canada). Goat anti-mouse alkaline phosphatase-conjugated antibody was from Invitrogen (Burlington, ON, Canada) and anti-EGFR antibody was from Santa Cruz Biotechnology (Santa Cruz, CA). Bisindolylmaleimide I (BIM), AG1478, mouse anti-phosphotyrosine (PY20) antibodies, and the phosphatase inhibitor cocktail set II were from Calbiochem (San Diego, CA) and urotensin II was from Phoenix Pharmaceutical (Belmont, CA). $^{125}$I-UII (specific radioactivity, 400 Ci/mmol) was prepared with IODO-GEN as described by Fraker and Speck (1978). In brief, 25 $\mu$l of 1 mM peptide solution was incubated with 20 $\mu$g of IODO-GEN (Pierce Chemical Co., Rockford, IL), 65 $\mu$l of 100 mM borate buffer, pH 8.5, and 1 mCi of Na$^{125}$I for 30 min at room temperature. The labeled peptides were purified by HPLC on a C-18 column (10 $\mu$m; Alltech Associates Inc., Deerfield, IL) with a 35 to 45% acetonitrile gradient. The specific radioactivity of the labeled hormones was determined by self-displacement and saturation binding analyses.

**PCR Mutagenesis.** Mutant UT receptor cDNAs were constructed by oligonucleotide-directed mutagenesis (Expand High Fidelity PCR System; Roche) using rat mycUT cDNA inserted into pcDNA3.1 (Invitrogen) as a template. Two sets of forward and reverse oligonucleotides were used to introduce mutations at Asp97$^{2.50}$, Glu147$^{3.49}$, Arg148$^{3.50}$, and Tyr149$^{3.51}$. PCR products were subcloned using KpnI and XbaI sites of pcDNA3.1 after digestion by the same restriction enzymes. Mutagenesis was confirmed by automated nucleotide sequencing.

**Cell Culture and Transfections.** COS-7 cells were grown in DMEM containing 10% (v/v) fetal bovine serum, 100 IU/ml penicillin, and 100 $\mu$g/ml streptomycin at 37°C. Cells ($1.2 \times 10^6$) were plated in 100-mm culture dishes. When they reached 70% confluence, they were transfected with 2 $\mu$g of plasmid DNA and 4 $\mu$l of FuGENE-6 according to the manufacturer's protocol. Transfected cells were grown for 48 h before performing binding assays. For confocal microscopy, HEK-293 cells were plated on 12-mm$^2$ coverslips in six-well plates at a density of $2.5 \times 10^5$ cells/well. When cells reached 70% confluence, they were transfected with 1 $\mu$g of receptor plasmid DNA/0.5 $\mu$g of $\beta$-arrestin2-GFP plasmid DNA and 2 $\mu$l of FuGENE-6 according to the manufacturer's protocol. Transfected cells were grown for 24 h, and images were captured using a Fluoview FV1000 confocal microscope (Olympus, Tokyo, Japan).

**Binding Experiments.** COS-7 cells were grown for 48 h after transfection in 100-mm culture dishes, washed once with PBS, and subjected to one freeze-thaw cycle. Broken cells were gently scraped in washing buffer (20 mM Tris-HCl, pH 7.4, and 5 mM $MgCl_2$), centrifuged at 2500*g* for 15 min at 4°C and resuspended in binding buffer (20 mM Tris-HCl, pH 7.4, 5 mM $MgCl_2$, 0.1% BSA, and 0.01% bacitracin). For saturation binding assays, broken cells (10–15 $\mu$g of protein) were incubated for 1 h at room temperature in binding buffer containing increasing concentrations of $^{125}$I-UII (0.15–20 nM, 50 Ci/mmol) in a final volume of 0.5 ml. Bound radioactivity was separated from free ligand by filtration through GF/C filters presoaked for at least 1 h in binding buffer. Nonspecific binding was measured in the presence of 1 $\mu$M unlabeled urotensin II. Receptor-bound radioactivity was evaluated by gamma counting. $K_d$ and $B_{max}$ values were evaluated using Prism version 5.00 for Windows (GraphPad Software, San Diego, CA). Peptide stability was evaluated by thin layer chromatography. No degradation was observed after incubating the peptide with COS-7 cell membranes for up to 2 h.

**Measurement of Agonist-Induced Inositol Phosphates.** Inositol phosphate (IP) accumulation was measured as described previously (Lanctot et al., 1999). In brief, COS-7 cells were seeded in six-well plates, transfected, and labeled for 16 h in serum-free, ino-

sitol-free DMEM containing 10 $\mu$Ci/ml of [*myo*-$H^3$]inositol (GE Healthcare, Chalfont St. Giles, Buckinghamshire, UK). Cells were washed twice with PBS supplemented with 0.1% dextrose and incubated in stimulation buffer (DMEM, 25 mM HEPES, pH 7.4, 10 mM LiCl, and 0.1% BSA) for 30 min at 37°C. Inositol phosphate production was induced by adding 0.1 $\mu$M urotensin II for 10 min at 37°C in stimulation buffer. Incubations were terminated by the addition of ice-cold perchloric acid [final 5% (v/v)]. Water-soluble IPs were extracted with an equal volume of a 1:1 mixture of 1,1,2-trichlorotrifluoroethane and tri-*n*-octylamine. The samples were vigorously mixed and centrifuged at 2500*g* for 30 min. The upper phase containing the IPs was applied to an AG1-X8 resin column (Bio-Rad Laboratories, Hercules, CA). The IPs were sequentially eluted with ammonium formate/formic acid solutions of increasing ionic strength. Fractions containing IPs were collected and radioactivity was measured using a liquid scintillation counter. Parallel plates were used to measure receptor expression and IP accumulation levels were adjusted based on receptor expression levels.

**Preparation of Cell Extracts and Immunoblotting.** Transfected COS-7 cells in 6-cm dishes were starved for 12 to 18 h in serum-free medium before stimulation. Where specified, protein kinase C inhibitor BIM alone or in combination with EGFR tyrosine kinase inhibitor AG1478 was added 30 min before UII. After stimulation, the medium was removed and cells were rinsed with ice-cold PBS. Cells were then lysed with 150 $\mu$l of radioimmunoprecipitation assay buffer (50 mM Tris, pH 7.5, 150 mM NaCl, 1% Nonidet P-40, 0.5% deoxycholic acid, 4 mM EDTA, and 0.1% SDS) containing protease inhibitor cocktail, 150 mM NaF, 50 mM sodium orthovanadate, and 250 mM $\beta$-glycerophosphate. Samples were centrifuged to remove insoluble material and protein concentrations were measured by Bradford assay. Proteins (40 $\mu$g) were resolved on 10% Tris/glycine polyacrylamide gels (Invitrogen) and transferred to nitrocellulose membranes for immunoblotting. Phosphorylated ERK1/2 and total ERK1/2 were detected by immunoblotting with rabbit polyclonal anti-phospho-p44/42 MAPK (1:2000; Cell Signaling Technology, Danvers, MA) and anti-MAP kinase (1:4000; Millipore, Billerica, MA) respectively. The antibodies were visualized with donkey anti-rabbit horseradish peroxidase antibodies (Bethyl Laboratories, Montgomery, TX) using Western Lightning Chemiluminescence Reagent Plus according to the manufacturer's instructions (PerkinElmer Life Sciences, Waltham, MA). Films were scanned, and band intensities were quantified using ImageJ software (http://rsb.info.nih.gov/ij/).

**EGFR Phosphorylation.** Transfected COS-7 cells in 10-cm dishes were starved for 12 to 18 h in serum-free medium before stimulation. Cells were then stimulated with UII (0.1 $\mu$M) or EGF (10 nM) for the indicated times, the medium was removed and cells were rinsed with ice-cold PBS. Cells were then lysed with 800 $\mu$l of lysis buffer (1% Triton X-100, 50 mM Tris, pH 7.5, 150 mM NaCl, and 4 mM EDTA) containing a protease inhibitor cocktail, a phosphatase inhibitor cocktail, 150 mM NaF, 50 mM sodium orthovanadate, and 250 $\mu$M $\beta$-glycerophosphate. Samples were centrifuged to remove insoluble material and protein concentrations were measured by Bradford assay. Equal amount of protein were immunoprecipitated using anti-EGFR antibodies. Western blots were probed sequentially with antiphosphotyrosine antibody (PY20) and the anti-EGFR antibody. The antibodies were visualized with specific secondary horseradish peroxidase antibodies (Bethyl Laboratories, Montgomery, TX) using Western Lightning Chemiluminescence Reagent Plus according to the manufacturer's instructions (PerkinElmer Life Sciences). Films were scanned and band intensities were quantified using ImageJ software (http://rsb.info.nih.gov/ij/).

**Enzyme-Linked Immunosorbent Assay.** Receptor internalization was quantified by ELISA as described elsewhere (Parent et al., 2001). In brief, COS-7 cells were seeded at $1.2 \times 10^6$ cells/100-mm dish and transfected with 2 $\mu$g of myc-UT or mutant cDNA in combination with 2 $\mu$g of pcDNA3.1 or $\beta$-arrestin2-GFP cDNA. Twenty-four hours after transfection, cells were transferred into six wells of a 24-well plate. The following day, the cells were washed once with PBS and incubated in the presence or the absence of 0.1 $\mu$M UII for 120 min at 37°C in prewarmed DMEM supplemented with 0.5% BSA and 20 mM HEPES, pH 7.4. The medium was then removed, the cells were fixed in 3.7% formaldehyde/TBS (20 mM Tris, pH 7.4, 150 mM NaCl) for 5 min at room temperature and washed three times with TBS. Nonspecific binding was blocked by incubating the cells in 1% TBS/BSA for 30 min. Anti-myc-specific monoclonal antibody (1:500 in TBS/BSA) was then added, and the incubation was continued for a further 60 min. Cells were then washed three times with TBS, blocked in TBS/BSA for 15 min and incubated with alkaline phosphatase-conjugated goat anti-mouse (1:1000 in TBS/BSA) for 60 min. Cells were then washed three times with TBS. *p*-Nitrophenyl-phosphate (250 $\mu$l) was added, and the plates were incubated at 37°C until a yellow color appeared (standardized at 45 min). A 100-$\mu$l aliquot was collected, neutralized by adding 100 $\mu$l of 0.4 N NaOH, and the absorbance was read at 405 nm using a Titertek Multiskan MCC/340 spectrophotometer. Cells transfected with pcDNA3.1 alone were used as controls. Results are shown as the percentage of cell surface receptor loss, where unstimulated cells represent 100% of receptor cell surface expression. To determine the expression levels of cell surface receptors, absorbance of unstimulated cells transfected with each receptor was measured and expressed as -fold absorbance over cells transfected with empty vector.

**Confocal Microscopy.** HEK-293 cells expressing myc-tagged UT (myc-UT) or mutant receptors and $\beta$-arrestin2-GFP were stimulated at 37°C with 0.1 $\mu$M UII for 30 min. They were then fixed for 30 min at room temperature in a solution of 3% (w/v) paraformaldehyde in PBS, permeabilized with 0.1% Triton X-100 for 10 min, and blocked with 1% BSA/PBS for 30 min. Cells were then incubated with anti-myc antibodies for 1 h at room temperature and then with Alexa Fluor 594-conjugated goat anti-mouse $F(ab')_2$ for 1 h. Coverslips were mounted on slides using Vectashield mounting medium (Vector Laboratories, Peterborough, UK).

Cells were examined with a scanning confocal microscope (FV1000; Olympus, Tokyo, Japan) coupled to an inverted microscope with a PlanApo 60×/1.42 oil immersion objective. Specimens were laser-excited at 488 nm (40-mW argon laser) for GFP and 543 nm (helium-neon laser) for Alexa Fluor 594. To avoid cross-talk between GFP and Alexa Fluor 594 fluorescence, readings were recorded sequentially at wavelengths ranging from 505 to 530 nm and 580 to 650 nm, respectively. Serial horizontal optical sections (1024 × 1024 pixels) with two-time line averaging were acquired. Olympus Fluoview software version 1.6a was used for image acquisition and analysis. The images were further processed using Adobe Photoshop (Adobe Systems, San Jose, CA).

**Data Analysis.** Results were collected in triplicate and are presented as means ± S.D. Binding curves, binding capacity ($B_{max}$) and $K_d$ values were determined using GraphPad Prism version 5.00 (GraphPad Software, San Diego CA). Statistical significance of the difference was assessed using one-way ANOVA and post hoc Dunnett test. *, $p < 0.05$; **, $p < 0.01$; ***, $p < 0.001$.

## Results

**Binding Properties of Wild-Type and Mutant UT Receptors.** To study the involvement of $Asp97^{2.50}$, $Glu147^{3.49}$, $Arg148^{3.50}$, and $Tyr149^{3.51}$ in the functionality of the UT receptor, we mutated the residues to alanine ($D97^{2.50}A$, $E147^{3.49}A$, $R148^{3.50}A$, and $Y149^{3.51}A$, respectively). Another mutant ($R148^{3.50}H$), which was based on a reported single nucleotide polymorphism of the UT receptor (refSNP ID rs13305975), was also constructed. To facilitate the comparison of residues in TMDs, amino acids were indexed according to their positions relative to the most conserved residue in the TMD (designated X.50, X being the TMD number) in

which they are located (Fig. 1) (Ballesteros and Weinstein, 1995).

To characterize the pharmacological properties of all mutants, binding analyses using increasing concentrations of $^{125}$I-UII (saturation kinetics) in transiently transfected COS-7 cells were used to characterize the pharmacological properties of the mutants. Table 1 shows that $K_d$ values ranged from 1.4 ± 0.2 nM (E147$^{3.49}$A) to 7.9 ± 2.3 nM (D97$^{2.50}$A), whereas expression levels ranged from 1.6 to 5.7 pmol/mg protein. ELISA analysis confirmed that mutant receptors were expressed at similar levels to those of wild-type receptor (Table 1).

**D97$^{2.50}$A and Arg148$^{3.50}$ Mutants Abolish Inositol Phosphate Accumulation.** To evaluate the functional properties of the wild-type and mutant receptors, we tested their capacity to activate G$\alpha_{q/11}$ by measuring UII-induced inositol phosphates accumulation. As shown in Fig. 2, 0.1 $\mu$M UII caused a significant inositol phosphate accumulation in COS-7 cells expressing the wild-type UT receptor. However, the effect of UII was significantly reduced in cells expressing the E147$^{3.49}$A and Y149$^{3.51}$A mutant receptors. Moreover, cells expressing the D97$^{2.50}$A or Arg148$^{3.50}$ mutant receptors did not accumulate inositol phosphates after UII stimulation. No constitutive activity was observed for any receptor tested as measured by inositol phosphate accumulation under basal conditions (data not shown).

**Arg148$^{3.50}$ Mutants Can Activate the MAPK Pathway.** UT receptor-mediated signaling activates the MAPK pathway, particularly by promoting extracellular-signal-regulated kinase 1/2 (ERK1/2) phosphorylation (Ziltener et al., 2002; Proulx et al., 2005). We previously reported that deleting specific residues in the carboxyl terminus of the UT receptor does not affect its ability to activate the ERK1/2 pathway (Proulx et al., 2005). In the present study, we measured the effect of Asp97$^{2.50}$ and ERY motif mutations on ERK1/2 activation by immunoblotting with antibodies directed against the phosphorylated active forms of ERK1/2 (p-ERK1/2). Addition of 0.1 $\mu$M UII to COS-7 cells transiently transfected with wild-type UT, E147$^{3.49}$A, or Y149$^{3.51}$A mutant receptors led to a robust activation of ERK1/2 after 2 and 30 min (Fig. 3, A and B). The D97$^{2.50}$A mutant did not activate ERK1/2 after UII stimulation. It is noteworthy that (unlike their inability to activate G$\alpha_{q/11}$) the R148$^{3.50}$A and R148$^{3.50}$H mutants were able to activate the MAPK pathway, although the temporal pattern of MAPK activation was altered. Indeed, very little ERK1/2 activation was observed after 2 min of UII stimulation whereas significant activation was detected after 30 min. The E147$^{3.49}$A and Y149$^{3.51}$A mutants exhibited a very slight but statistically significant increase of the basal phosphorylation of ERK1/2 that may represent constitutive activity of these mutants toward MAPK activation (Fig. 3B).

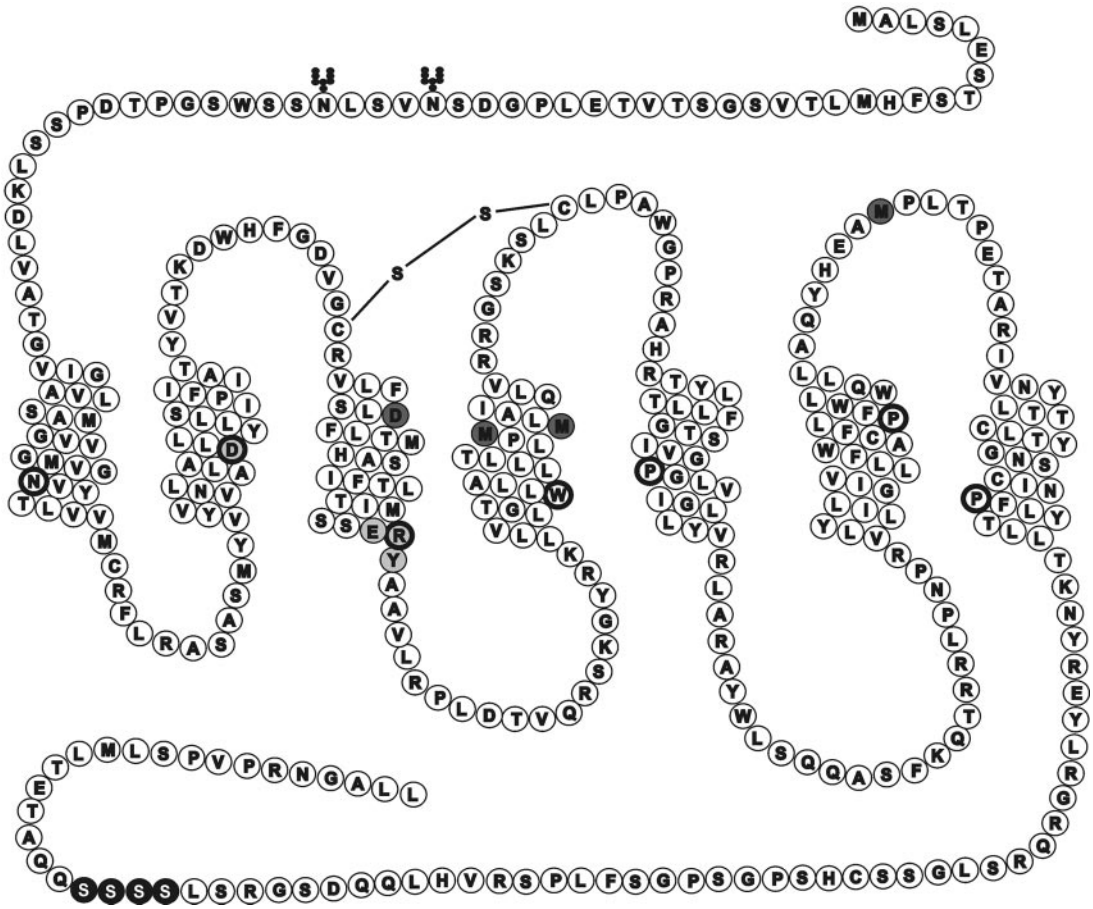

**Fig. 1.** Schematic representation of the rat wild-type UT receptor (386 amino acids) and mutant receptors (light gray) in which Asp97$^{2.50}$, Glu147$^{3.49}$, Arg148$^{3.50}$, and Tyr149$^{3.51}$ were replaced by alanine or histidine (R148$^{3.50}$H). The most conserved residues of each TMD are circled in bold. Residues of the UT receptor that are important for UII binding are in dark gray (Boucard et al., 2003; Holleran et al., 2007), and those that are important for internalization are in black with white lettering (Proulx et al., 2005). Putative Asn-glycosylation sites (Asn$^{29}$, Asn$^{33}$) and the conserved disulfide bridge are depicted.

**UT-Dependent Activation of ERK1/2 Involves Both PKC and Transactivation of the EGF Receptor.** Because the G protein-mediated activity of UII is typically transduced by $G\alpha_{q/11}$ leading to PKC activation, we evaluated the extent of PKC dependence on ERK1/2 activation in COS-7 cells transfected with the UT receptor. Moreover, EGFR-dependent ERK1/2 activation by the UT receptor has been reported in cardiomyocytes (Onan et al., 2004). To determine the contribution of PKC- and EGFR-dependent mechanisms to ERK1/2 activation, cells were pretreated either with 1 $\mu$M BIM, a PKC inhibitor, or with 0.5 $\mu$M AG1478, an EGFR kinase inhibitor, or simultaneously with both inhibitors before evaluating the temporal pattern of ERK1/2 activation by UII. In untreated COS-7 cells transfected with the UT receptor, 0.1 $\mu$M UII promoted a specific temporal ERK1/2 activation pattern (Fig. 4, A and B). Early rapid activation of ERK1/2 was observed at 2 to 5 min, peaking at 5 min followed by a slow decrease toward basal levels (30 min). BIM-mediated PKC inhibition reduced early ERK1/2 activation but did not affect late ERK1/2 activation (10–30 min). On the other hand, AG1478 reduced ERK activation at each time point, but early activation (2–5 min) was maintained. The addition of both BIM and AG1478 almost entirely abolished the ability of the UT receptor to promote ERK1/2 phosphorylation, suggesting that the PKC- and EGFR-dependent pathways play a major role in ERK1/2 activation by UT. These results suggest that PKC activation and EGFR transactivation are the main ERK-activation pathways in COS-7 cells after UT receptor activation. They also revealed the important contribution of PKC to UII-induced phosphorylation of ERK1/2 at the early time points.

**$Arg148^{3.50}$ Mutants Transactivate EGFR via a $G\alpha_{q/11}$-Independent Mechanism.** To better understand how the $Arg148^{3.50}$ mutants promoted ERK1/2 phosphorylation, we determined the temporal pattern of ERK1/2 activation by $R148^{3.50}A$ and $R148^{3.50}H$. Figure 4, C and D, showed that the $Arg148^{3.50}$ mutants promoted ERK1/2 activation but that the activation was delayed. This suggests that these mutants, because they are unable to activate the $G\alpha_{q/11}$-PLC pathway, promote ERK1/2 phosphorylation by transactivating EGFR. This is supported by the fact that AG1478 entirely abolished UII-induced ERK1/2 phosphorylation in cells expressing the $R148^{3.50}A$ and $R148^{3.50}H$ mutants (Fig. 4, C and D). To confirm that the $Arg148^{3.50}$ mutants were able to promote EGFR transactivation, COS-7 cells transiently transfected with wild-type UT receptor or $Arg148^{3.50}$ mutant constructs were stimulated with UII and lysed. Presence of active tyrosine-phosphorylated EGFR was then confirmed with anti-phosphotyrosine antibodies (anti-p-Tyr). Figure 4E shows that activated UT receptor, as well as both $Arg148^{3.50}$ mutants, promoted the tyrosine phosphorylation of EGFR. Moreover, this transactivation was delayed in cells expressing the $Arg148^{3.50}$ mutants (Fig. 4, E and F). These results suggest that $Arg148^{3.50}$ of the ERY motif is essential for the activation of $G\alpha_{q/11}$ but is not involved in the transactivation of EGFR and that the UT receptor activates two independent mechanisms that lead to ERK1/2 phosphorylation.

**Role of $Asp97^{2.50}$, $Glu147^{3.49}$, $Arg148^{3.50}$, and $Tyr149^{3.51}$ in Agonist-Dependent Cell Surface Receptor Loss.** We showed previously that UT undergoes agonist-induced internalization in COS-7 cells (Proulx et al., 2005). Figure 5 shows that a 2-hour treatment with 0.1 $\mu$M UII caused a significant 20% loss of cell surface receptors on cells expressing the UT receptor. Under the same conditions, the $D97^{2.50}A$ and both $Arg148^{3.50}$ mutant receptors showed no significant loss of cell surface receptors, whereas the $Y149^{3.51}A$ mutant behaved as wild-type receptor. It is noteworthy that the agonist-induced cell surface loss of $E149^{3.49}A$ receptors increased considerably compared with wild-type receptor. To determine whether this was modulated by arrestins, we coexpressed $\beta$-arrestin2-GFP with the wild-type and mutant receptors. As shown in Fig. 5 (black columns), coexpression of $\beta$-arrestin2-GFP increased cell sur-

TABLE 1

Affinities and expression levels of UT receptor mutants in transiently transfected COS-7 cells

Saturation-binding studies with broken cells expressing wild-type or mutant receptors were carried out as described under *Materials and Methods*. $B_{max}$ and $K_d$ values were determined using GraphPad Prism version 5.00 for Windows. Relative expression of wild-type and mutant receptors was determined by ELISA (-fold absorbance over mock-transfected cells). Results are the means of three to five separate experiments.

| Receptor | $K_d$[a] | $B_{max}$ | Cell Surface Expression |
|---|---|---|---|
| | *nM* | *pmol/mg protein* | |
| UT | 3.8 ± 1.9 | 3.2 ± 1.6 | 6.0 ± 1.3 |
| $D97^{2.50}A$ | 7.9 ± 2.3 | 3.3 ± 2.6 | 6.1 ± 1.5 |
| $E147^{3.49}A$ | 1.4 ± 0.2 | 1.6 ± 0.6 | 4.0 ± 0.9 |
| $R148^{3.50}A$ | 5.6 ± 1.4 | 4.7 ± 4.4 | 6.3 ± 1.5 |
| $R148^{3.50}H$ | 4.7 ± 2.4 | 5.6 ± 3.0 | 5.9 ± 1.8 |
| $Y149^{3.51}A$ | 3.1 ± 0.5 | 1.8 ± 1.0 | 5.8 ± 1.4 |

TABLE 2

Summary of results obtained with wild-type and mutant receptors

| Receptor | IPs | ERK1/2 | EGFR Transactivation | Cell Surface Receptor Loss | Co-localized $\beta$-arr2-GFP |
|---|---|---|---|---|---|
| UT | + | + | + | + | + |
| $D97^{2.50}A$ | − | − | N.D. | − | − |
| $E147^{3.49}A$ | + | + | N.D. | + | + |
| $R148^{3.50}A$ | − | + | + | − | − |
| $R148^{3.50}H$ | − | + | + | − | − |
| $Y149^{3.51}A$ | + | + | N.D. | + | + |

+, functional response; −, no functional response; N.D., not determined.

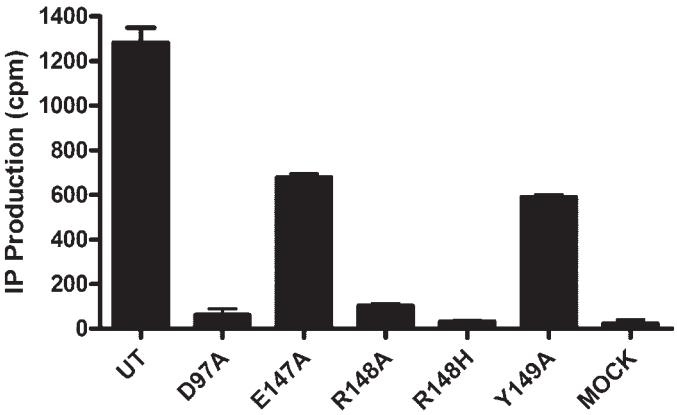


**Fig. 2.** Inositol phosphate production by the wild-type and mutant receptors. Inositol phosphate production was evaluated in COS-7 cells transfected with wild-type or mutant receptors. Inositol phosphate production was induced with 0.1 $\mu$M UII for 10 min at 37°C in stimulation buffer. The incubation was stopped with perchloric acid, and inositol phosphate levels were measured as described under *Materials and Methods*. Results are the sum of the amounts of inositol bisphosphate, inositol trisphosphate, and inositol tetrakisphosphate in excess of the basal level and are expressed as mean experimental variations of triplicate values. The results are representative of four independent experiments.

face receptor loss of wild-type, E147$^{3.49}$A, and Y149$^{3.51}$A mutant receptors by 100, 54, and 102%, respectively, but did not significantly affect the cell surface loss of the D97$^{2.50}$A or Arg148$^{3.50}$ mutants.

**Asp97$^{2.50}$ and Arg148$^{3.50}$ Mutants Do Not Promote β-Arrestin Translocation.** We reported previously that activated UT receptors traffic into intracellular vesicles in HEK-293 cells and colocalize with either β-arrestin1-YFP or β-arrestin2-GFP (Proulx et al., 2005). To determine whether activated mutant receptors were able to promote β-arrestin translocation, we coexpressed myc-tagged wild-type and mutant receptors with functional conjugated

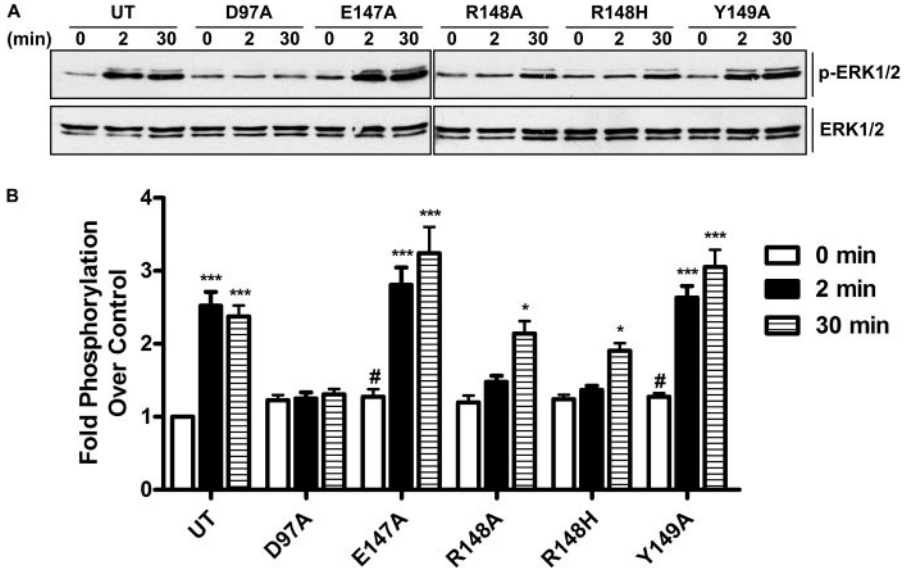


**Fig. 3.** Effect of UT receptor mutations on MAPK activation. COS-7 cells transiently transfected with either wild-type or mutant receptors were serum-starved overnight. They were then treated with 0.1 μM UII at 37°C for 0, 2, or 30 min in DMEM and lysed. Equal amounts of protein were resolved by SDS/PAGE. A, activated MAPK was identified by immunoblotting using phospho-MAPK specific antibody, which labeled the 44- and 42-kDa bands (ERK1 and ERK2, respectively). The total amount of MAPK was the same in all samples based on parallel blots probed with antibody directly against total MAPK. B. *p*-ERK1/2 bands were analyzed by densitometry and presented as -fold phosphorylation (mean ± S.E.M. $n = 3$) over UT basal. Statistical significance of the difference was assessed using one-way ANOVA and post hoc Dunnett test. ∗, $p < 0.05$; ∗∗∗, $p < 0.001$. # represents statistically significant differences ($p < 0.05$) of basal phosphorylation of mutants compared with basal phosphorylation of wild-type UT.

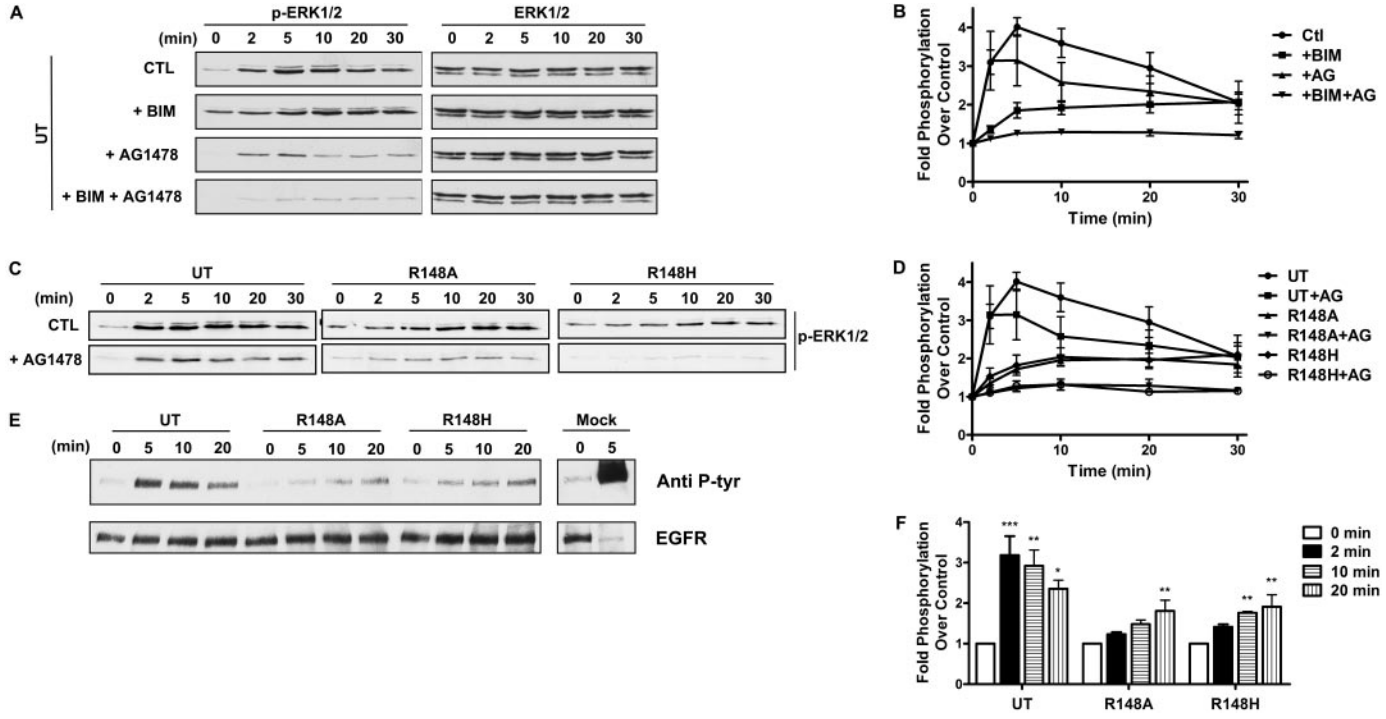


**Fig. 4.** Arg148$^{3.50}$ mutants promote ERK1/2 activation by transactivation of EGFR. COS-7 cells transiently transfected with wild-type receptor (A) or Arg148 mutants (C) were serum-starved overnight. They were then treated with 1 μM BIM and/or 0.5 μM AG1478 for 30 min, stimulated with 0.1 μM UII at 37°C for the indicated time in DMEM, and lysed. Equal amounts of protein were resolved by SDS/PAGE. Activated MAPK was identified by immunoblotting using phospho-MAPK-specific antibody, which labeled the 44- and 42-kDa bands (ERK1 and ERK2, respectively). The total amount of MAPK was the same in all samples based on parallel blots probed with antibody directed against total MAPK. B and D, *p*-ERK1/2 bands were analyzed by densitometry and presented as -fold phosphorylation (mean ± S.E.M. $n = 3$) over basal as reference. E, COS-7 cells transiently transfected with wild-type receptor, or Arg148$^{3.50}$ mutants were serum-starved overnight. They were then stimulated with 0.1 μM UII at 37°C for the indicated time in DMEM and lysed. The EGFR was immunoprecipitated from cell extracts and Western blotted using antibodies for phosphotyrosine and total EGFR protein. F, *p*-Tyr-EGFR bands were analyzed by densitometry and presented as -fold phosphorylation (mean ± S.E.M. $n = 3$) over basal. Statistical significance of the difference was assessed using one-way ANOVA and post hoc Dunnett test. ∗, $p < 0.05$; ∗∗, $p < 0.01$; ∗∗∗, $p < 0.001$.

β-arrestin2-GFP in HEK-293 cells. Under control conditions, UT was localized to the plasma membrane (Fig. 6A), whereas β-arrestin2-GFP was uniformly distributed in the cell cytosol. After exposure to agonist (30 min), both UT and β-arrestin2-GFP redistributed to vesicular structures of the cell, and UT colocalized with β-arrestin2-GFP (Fig. 6A, merged images). Under the same experimental conditions, D97$^{2.50}$A and Arg148$^{3.50}$ mutants were also distributed in the plasma membrane under basal conditions, but exposure to UII modified neither their distribution nor the cytosolic distribution of β-arrestin2-GFP (Fig. 6B). However, E147$^{3.49}$A and Y149$^{3.51}$A behaved like the wild-type receptor distributing at the plasma membrane under control conditions and colocalizing with β-arrestin2-GFP in vesicular structure after exposure to UII.

## Discussion

The aim of this study was to determine the role of the conserved residues/motif Asp$^{2.50}$ and ERY on the functionality of the UT receptor. Five mutants were constructed, all of which displayed cell-surface expression levels and binding properties toward the natural ligand, UII, that were similar to that of the wild-type receptor, which suggests that the mutations did not significantly perturb the overall structure of the receptor.

Substitution of Asp$^{2.50}$ in TMD2 by alanine in the UT receptor (D97$^{2.50}$A) led to a receptor that could no longer activate phospholipase C with ensuing lack of inositol phosphate production (Table 2). UII binding neither promoted loss of cell surface of the D97$^{2.50}$A receptor nor activated the MAPK pathway. Asp$^{2.50}$ played a major role in the activation of class A GPCRs because mutations of this residue alter the signaling capacity of many GPCRs (Neve et al., 1991; Bihoreau et al., 1993). An interaction between Asp$^{2.50}$ and the conserved Asn$^{7.49}$ of the NPxxY motif in TMD7 may be important in the activation mechanism of GPCRs (Sealfon et al., 1995; Urizar et al., 2005). Asn$^{7.49}$ acts as an on/off switch by adopting different orientations in the inactive and active states (Govaerts et al., 2001; Urizar et al., 2005). In the inactive state, Asn$^{7.49}$ is restrained toward TMD6, whereas in the active state, it probably adopts an orientation favoring an interaction with Asp$^{2.50}$ (Urizar et al., 2005). Altering Asp$^{2.50}$ in the UT receptor would abrogate an obligatory interaction with Asn$^{7.49}$ in TMD7 needed to maintain the active state. Like other class A GPCRs, substituting the Asp$^{2.50}$ residue in the UT receptor with another amino acid would profoundly affect the ability of the receptor to transit from an inactive to an active state upon agonist binding.

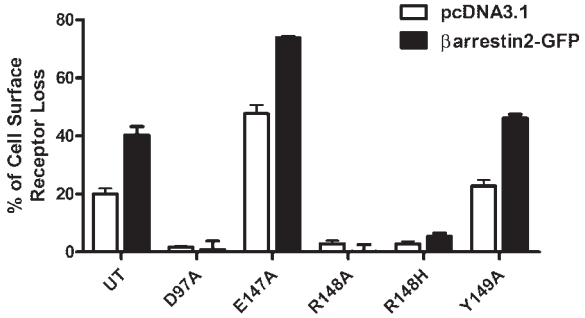


**Fig. 5.** Agonist-dependent cell surface receptor loss of wild-type and mutant receptors. COS-7 cells expressing myc-tagged UT or mutant receptors cotransfected with pcDNA3.1 or β-arrestin2-GFP were stimulated with 0.1 μM UII for 120 min. Cell surface receptor loss was quantified by ELISA as described under *Materials and Methods*. Mock-transfected cells were used to determine background. Results are the means ± S.E.M of four independent experiments.

In many GPCRs, including rhodopsin, mutating Glu or Asp in the E/D$^{3.49}$RY motif to either Ala or Asn might eliminate an ionic interaction with Arg$^{3.50}$ and increase their constitutive activity (Mhaouty-Kodja et al., 1999; Alewijnse et al., 2000; Ballesteros et al., 2001). However, for some GPCRs, E/D$^{3.49}$ substitutions do not induce constitutive activation, suggesting that this residue has other roles (Ohyama et al., 2002; Capra et al., 2004). Using inositol phosphate production as a functional assay, replacing Glu147$^{3.49}$ with alanine (E147$^{3.49}$A) in the UT receptor did not promote constitutive activation. Thus, a putative ionic interaction between Glu147$^{3.49}$ and Arg148$^{3.50}$ would not constitute a major determinant in maintaining basal state of UT.

The E147$^{3.49}$A mutant exhibited two particular properties. First, activating this mutant did not produce a maximal response compared with the wild-type receptor and, second, the agonist-dependent cell surface loss was greater than the wild-type receptor. It is thus possible that the reduced signaling efficacy of E147$^{3.49}$A may be due to structural changes in the activated receptor that influence $G\alpha_{q/11}$ protein coupling and/or that enable increased coupling to the internalization machinery thereby increasing its desensitization relative to the wild-type receptor.

As mentioned above, we observed that, after agonist binding, loss at the cell surface of the E147$^{3.49}$A mutant was greater compared with the wild-type receptor, a process that was improved by overexpressing β-arrestin2 (similar results were obtained with β-arrestin1; data not shown), which points to a β-arrestin-dependent internalization mechanism. Marion at al. recently proposed a model whereby the proximal 10 residues of second intracellular loops, including the E/DRY motif in rhodopsin-like receptors, provide binding determinants for β-arrestin recognition (Marion et al., 2006). The highly conserved amino acids proline and alanine, which reside six residues at the C terminus of the E/DRY motif, regulate β-arrestin binding and β-arrestin-mediated internalization. It has been suggested that a conformational change directed by the second intracellular loop, probably using the loop itself as a binding patch, functions as a switch for transitioning β-arrestin from its inactive form to its active receptor-binding state. Replacing Glu147$^{3.49}$ in the UT receptor may thus influence the orientation of residues of the second intracellular loop, which is involved in recognizing β-arrestins and modulating the affinity of the activated receptor to β-arrestins. Our results thus suggest that residue Glu147$^{3.49}$ plays an important role in the contribution of the second intracellular loop of the UT receptor to the internalization of the receptor. However, because our method using ELISAs reveals loss of cell-surface receptors after agonist stimulation, we cannot exclude the possibility that trafficking, degradation, and recycling processes may affect the overall cell surface expression of the Glu147$^{3.49}$ mutant.

An analysis of the activation profile of the MAPK pathway using the wild-type UT receptor reveals an early PKC-dependent pathway and an EGFR-dependent pathway that are involved in the activation of ERK1/2 in COS-7 cells. These

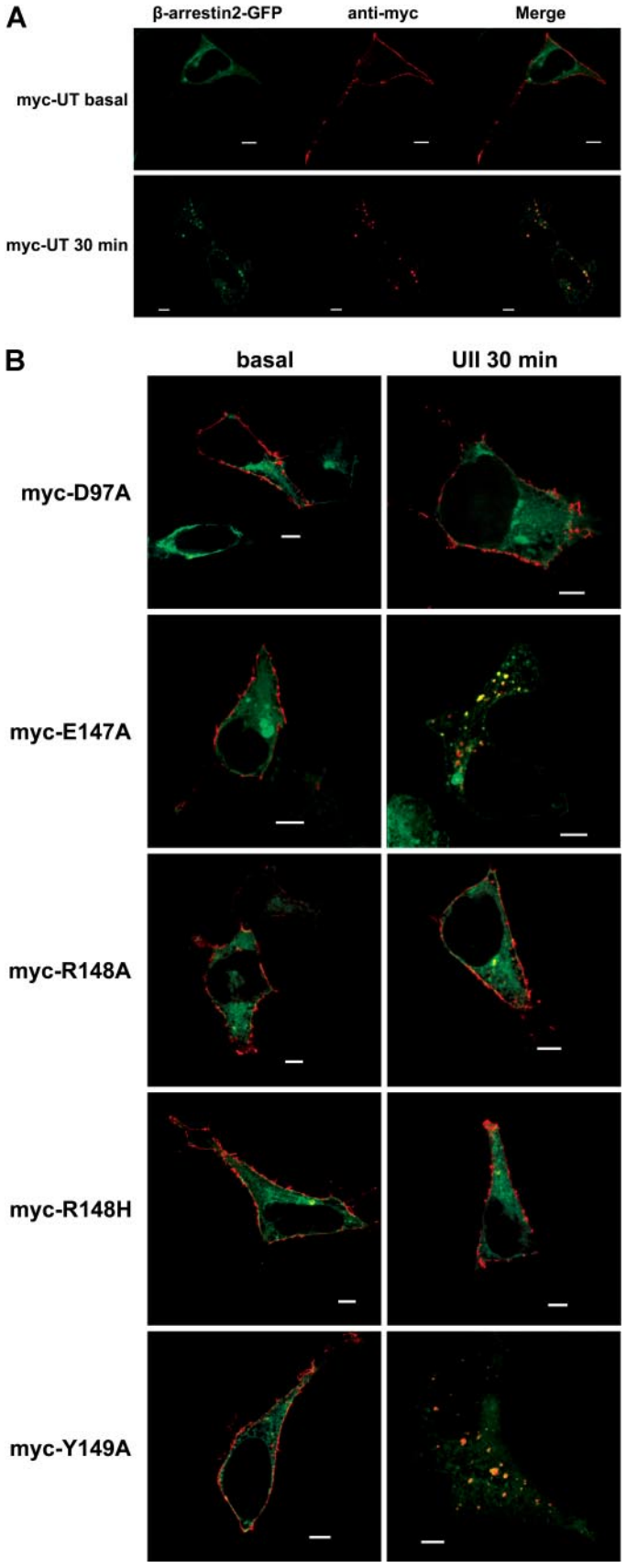


**Fig. 6.** Colocalization of β-arrestin2 with agonist-activated UT and mutant receptors. HEK-293 cells were transiently transfected with either myc-UT (A) or myc-tagged mutant receptors (B) together with β-arrestin2-GFP. Shown are representative confocal microscopic images of either myc-UT or myc-tagged mutants and β-arrestin2-GFP fluorescence in HEK-293 cells treated with agonist for 30 min at 37°C as described under *Materials and Methods*. Scale bars, 5 μm. Experiments were repeated three times with similar results.

two pathways probably mediate the signaling profile of the UT receptor toward ERK1/2 activation, because inhibiting PKC and EGFR abolished ERK1/2 activation altogether. Substituting the conserved residue Arg148$^{3.50}$ by alanine or histidine completely abolished the ability of the UT receptor to promote $G\alpha_{q/11}$ activation/inositol phosphate accumulation and abrogated the internalization of the receptor in COS-7 cells after UII binding. In HEK-293 cells, the Arg148$^{3.50}$ mutants did not promote β-arrestin2-GFP translocation or colocalization to UII-bound receptors. However, UII binding to R148$^{3.50}$A and R148$^{3.50}$H mutants induced ERK1/2 activation at later (30 min) but not earlier (2 min) time points. This activation was abolished by the addition of AG1478, an EGFR kinase inhibitor. Moreover, stimulated Arg148$^{3.50}$ mutants promoted EGFR activation as demonstrated in Fig. 4, E and F. This suggests that the R148$^{3.50}$A and R148$^{3.50}$H mutants, which are unable to promote the phospholipase C/inositol phosphate/PKC activation cascade, can still activate ERK1/2 in a $G\alpha_{q/11}$ protein-independent manner by transactivation of EGFR. ERK1/2 activation by GPCRs involves a complex network of G protein-dependent and -independent signals (Luttrell, 2003). For example, the angiotensin II type 1A ($AT_1$) receptor in HEK-293 cells activates ERK1/2 by distinct pathways, either G protein or β-arrestin dependent (Ahn et al., 2004). Moreover, $G\alpha_{q/11}$-independent signaling via EGFR transactivation as the main transductional mechanism for ERK1/2 activation has also been described for $AT_1$ in CHO-K1 and in human coronary artery smooth muscle cells (Miura et al., 2004). In the case of the UT receptor, the fact that the Arg148$^{3.50}$ mutants maintained their ability to activate ERK1/2 but were unable to recruit β-arrestin suggests that ERK1/2 activation is β-arrestin-independent.

Mutations in the DRY motif of other GPCRs such as the angiotensin II $AT_1$ receptor overexpressed in the hearts of transgenic mice cause cardiac hypertrophy (Zhai et al., 2005), lending weight to the importance of this motif in GPCR function. In addition, an Arg$^{3.50}$-to-His mutation in the vasopressin V2 receptor (V2R) has been shown to lead to a constitutively phosphorylated receptor (R137HV2R) that associates with β-arrestins and is sequestered in intracellular vesicles, thus behaving as a constitutively desensitized receptor (Barak et al., 2001). This mutated receptor has been associated with nephrogenic diabetes insipidus (Bichet, 1998), R137HV2R acting as a loss-of-function receptor (Barak et al., 2001). These observations, along with our results on the R148$^{3.50}$H receptor, are of particular interest in light of a reported single nucleotide polymorphism (refSNP ID rs13305975) replacing Arg$^{3.50}$ with His. Whether this polymorphism is linked to or could be a marker of a specific pathology remains to be addressed.

The urotensin II system has been implicated in the development of pathophysiological conditions such as cardiac hypertrophy (Tzanidis et al., 2003), which involves EGFR transactivation in cardiomyocytes (Onan et al., 2004). Whether UT receptor activation in a normal or mutated genetic background promotes cardiac hypertrophy via a

$G\alpha_{q/11}$-independent mechanism involving EGFR transactivation, as observed for the $AT_1$ receptor, remains to be confirmed.

The $Tyr^{3.51}$ residue is the least conserved and studied residue of the E/DRY motif; cysteinyl, histidyl, and serine residues occur in some GPCRs. Tyrosine residue mutations often do not affect (Gáborik et al., 2001) or only marginally affect (Hawtin, 2005) receptor function. The substitution of $Tyr^{3.51}$ with alanine did not significantly alter the functionality of the UT receptor and led to only a small decrease in inositol phosphate production.

In light of various analyses of mutations, two roles have been proposed for the E/DRY motif in class A GPCRs (Rovati et al., 2007). In a first group of receptors, E/DRY would be involved in constraining GPCRs in their inactive ground state. Within this group, nonconservative $E/D^{3.49}$ mutations induce constitutive activity, whereas $Arg^{3.50}$ mutations have variable effects on receptor functions. In the second group, the motif would be involved in mediating G protein coupling/recognition, because $E/D^{3.49}$ mutations do not induce constitutive activity. However, nonconservative E/D mutations have multiple effects, indicating that this motif plays an important role in stabilizing the conformation of the receptor (Rovati et al., 2007). Moreover, nonconservative $Arg^{3.50}$ mutations invariably exert strongly disruptive effects on receptor activity and decrease agonist affinity, indicating that $Arg^{3.50}$ is involved in receptor-G protein-coupling/recognition. In light of results obtained in the present study, the ERY motif in the UT receptor can be considered a major determinant involved in shifting the receptor to an active conformation after urotensin II binding and may thus promote G protein coupling/recognition/activation rather than constrain the receptor in its ground state. An in-depth analysis of the ERY motif of the UT receptor will be needed to better clarify its role in receptor function.

**References**


Ahn S, Shenoy SK, Wei H, and Lefkowitz RJ (2004) Differential kinetic and spatial patterns of β-arrestin and G protein-mediated ERK activation by the angiotensin II receptor. *J Biol Chem* **279:**35518–35525.

Alewijnse AE, Timmerman H, Jacobs EH, Smit MJ, Roovers E, Cotecchia S, and Leurs R (2000) The effect of mutations in the DRY motif on the constitutive activity and structural instability of the histamine $H_2$ receptor. *Mol Pharmacol* **57:**890–898.

Ames RS, Sarau HM, Chambers JK, Willette RN, Aiyar NV, Romanic AM, Louden CS, Foley JJ, Sauermelch CF, Coatney RW, et al. (1999) Human urotensin-II is a potent vasoconstrictor and agonist for the orphan receptor GPR14. *Nature* **401:** 282–286.

Arnis S, Fahmy K, Hofmann KP, and Sakmar TP (1994) A conserved carboxylic acid group mediates light-dependent proton uptake and signaling by rhodopsin. *J Biol Chem* **269:**23879–23881.

Ballesteros JA, Jensen AD, Liapakis G, Rasmussen SG, Shi L, Gether U, and Javitch JA (2001) Activation of the $\beta_2$-adrenergic receptor involves disruption of an ionic lock between the cytoplasmic ends of transmembrane segments 3 and 6. *J Biol Chem* **276:**29171–29177.

Ballesteros JA and Weinstein H (1995) Integrated methods for the construction of three-dimensional models and computational probing of structure-function relations in G protein-coupled receptors, in *Receptor Molecular Biology* (Sealfon SC ed) vol. 25, pp. 366–428, Academic Press, San Diego, CA.

Barak LS, Oakley RH, Laporte SA, and Caron MG (2001) Constitutive arrestin-mediated desensitization of a human vasopressin receptor mutant associated with nephrogenic diabetes insipidus. *Proc Natl Acad Sci U S A* **98:**93–98.

Bichet DG (1998) Nephrogenic diabetes insipidus. *Am J Med* **105:**431–442.

Bihoreau C, Monnot C, Davies E, Teutsch B, Bernstein KE, Corvol P, and Clauser E (1993) Mutation of Asp74 of the rat angiotensin II receptor confers changes in antagonist affinities and abolishes G-protein coupling. *Proc Natl Acad Sci U S A* **90:**5133–5137.

Bockaert J and Pin JP (1999) Molecular tinkering of G protein-coupled receptors: an evolutionary success. *EMBO J* **18:**1723–1729.

Boucard AA, Sauvé SS, Guillemette G, Escher E, and Leduc R (2003) Photolabelling the rat urotensin II/GPR14 receptor identifies a ligand-binding site in the fourth transmembrane domain. *Biochem J* **370:**829–838.

Capra V, Veltri A, Foglia C, Crimaldi L, Habib A, Parenti M, and Rovati GE (2004) Mutational analysis of the highly conserved ERY motif of the thromboxane $A_2$ receptor: alternative role in G protein-coupled receptor signaling. *Mol Pharmacol* **66:**880–889.

Chung DA, Wade SM, Fowler CB, Woods DD, Abada PB, Mosberg HI, and Neubig RR (2002) Mutagenesis and peptide analysis of the DRY motif in the alpha2A adrenergic receptor: evidence for alternate mechanisms in G protein-coupled receptors. *Biochem Biophys Res Commun* **293:**1233–1241.

Douglas SA, Dhanak D, and Johns DG (2004) From 'gills to pills': urotensin-II as a regulator of mammalian cardiorenal function. *Trends Pharmacol Sci* **25:**76–85.

Douglas SA, Sulpizio AC, Piercy V, Sarau HM, Ames RS, Aiyar NV, Ohlstein EH, and Willette RN (2000) Differential vasoconstrictor activity of human urotensin-II in vascular tissue isolated from the rat, mouse, dog, pig, marmoset and cynomolgus monkey. *Br J Pharmacol* **131:**1262–1274.

Feng W and Song ZH (2003) Effects of D3.49A, R3.50A, and A6.34E mutations on ligand binding and activation of the cannabinoid-2 (CB2) receptor. *Biochem Pharmacol* **65:**1077–1085.

Fraker PJ and Speck JC Jr (1978) Protein and cell membrane iodinations with a sparingly soluble chloroamide, 1,3,4,6-tetrachloro-3a,6a-diphrenylglycoluril. *Biochem Biophys Res Commun* **80:**849–857.

Gáborik Z, Szaszák M, Szidonya L, Balla B, Paku S, Catt KJ, Clark AJ, and Hunyady L (2001) β-Arrestin- and dynamin-dependent endocytosis of the AT1 angiotensin receptor. *Mol Pharmacol* **59:**239–247.

Gether U, Lin S, Ghanouni P, Ballesteros JA, Weinstein H, and Kobilka BK (1997) Agonists induce conformational changes in transmembrane domains III and VI of the beta2 adrenoceptor. *EMBO J* **16:**6737–6747.

Govaerts C, Lefort A, Costagliola S, Wodak SJ, Ballesteros JA, Van Sande J, Pardo L, and Vassart G (2001) A conserved Asn in transmembrane helix 7 is an on/off switch in the activation of the thyrotropin receptor. *J Biol Chem* **276:**22991–22999.

Hawtin SR (2005) Charged residues of the conserved DRY triplet of the vasopressin V1a receptor provide molecular determinants for cell surface delivery and internalization. *Mol Pharmacol* **68:**1172–1182.

Holleran BJ, Beaulieu ME, Proulx CD, Lavigne P, Escher E, and Leduc R (2007) Photolabelling the urotensin II receptor reveals distinct agonist- and partial-agonist-binding sites. *Biochem J* **402:**51–61.

Lanctôt PM, Leclerc PC, Escher E, Leduc R, and Guillemette G (1999) Role of N-glycosylation in the expression and functional properties of human AT1 receptor. *Biochemistry* **38:**8621–8627.

Luttrell LM (2003) 'Location, location, location': activation and targeting of MAP kinases by G protein-coupled receptors. *J Mol Endocrinol* **30:**117–126.

Marion S, Oakley RH, Kim KM, Caron MG, and Barak LS (2006) A β-arrestin binding determinant common to the second intracellular loops of rhodopsin family G protein-coupled receptors. *J Biol Chem* **281:**2932–2938.

Mhaouty-Kodja S, Barak LS, Scheer A, Abuin L, Diviani D, Caron MG, and Cotecchia S (1999) Constitutively active alpha 1b adrenergic receptor mutants display different phosphorylation and internalization features. *Mol Pharmacol* **55:**339–347.

Miura S, Zhang J, Matsuo Y, Saku K, and Karnik SS (2004) Activation of extracellular signal-activated kinase by angiotensin II-induced Gq-independent epidermal growth factor receptor transactivation. *Hypertens Res* **27:**765–770.

Neve KA, Cox BA, Henningsen RA, Spanoyannis A, and Neve RL (1991) Pivotal role for aspartate-80 in the regulation of dopamine D2 receptor affinity for drugs and inhibition of adenylyl cyclase. *Mol Pharmacol* **39:**733–739.

Ohyama K, Yamano Y, Sano T, Nakagomi Y, Wada M, and Inagami T (2002) Role of the conserved DRY motif on G protein activation of rat angiotensin II receptor type 1A. *Biochem Biophys Res Commun* **292:**362–367.

Onan D, Pipolo L, Yang E, Hannan RD, and Thomas WG (2004) Urotensin II promotes hypertrophy of cardiac myocytes via mitogen-activated protein kinases. *Mol Endocrinol* **18:**2344–2354.

Overington JP, Al-Lazikani B, and Hopkins AL (2006) How many drug targets are there? *Nat Rev Drug Discov* **5:**993–996.

Palczewski K, Kumasaka T, Hori T, Behnke CA, Motoshima H, Fox BA, Le Trong I, Teller DC, Okada T, Stenkamp RE, et al. (2000) Crystal structure of rhodopsin: A G protein-coupled receptor. *Science* **289:**739–745.

Parent JL, Labrecque P, Driss Rochdi M, and Benovic JL (2001) Role of the differentially spliced carboxyl terminus in thromboxane A2 receptor trafficking: identification of a distinct motif for tonic internalization. *J Biol Chem* **276:**7079–7085.

Proulx CD, Simaan M, Escher E, Laporte SA, Guillemette G, and Leduc R (2005) Involvement of a cytoplasmic-tail serine cluster in urotensin II receptor internalization. *Biochem J* **385:**115–123.

Rosenbaum DM, Cherezov V, Hanson MA, Rasmussen SG, Thian FS, Kobilka TS, Choi HJ, Yao XJ, Weis WI, Stevens RC, et al. (2007) GPCR engineering yields high-resolution structural insights into beta2-adrenergic receptor function. *Science* **318:**1266–1273.

Rovati GE, Capra V, and Neubig RR (2007) The highly conserved DRY motif of class A G protein-coupled receptors: beyond the ground state. *Mol Pharmacol* **71:**959–964.

Saetrum Opgaard O, Nothacker H, Ehlert FJ, and Krause DN (2000) Human urotensin II mediates vasoconstriction via an increase in inositol phosphates. *Eur J Pharmacol* **406:**265–271.

Scheer A, Fanelli F, Costa T, De Benedetti PG, and Cotecchia S (1996) Constitutively active mutants of the alpha 1B-adrenergic receptor: role of highly conserved polar amino acids in receptor activation. *EMBO J* **15:**3566–3578.

Sealfon SC, Chi L, Ebersole BJ, Rodic V, Zhang D, Ballesteros JA, and Weinstein H (1995) Related contribution of specific helix 2 and 7 residues to conformational activation of the serotonin 5-HT2A receptor. *J Biol Chem* **270:**16683–16688.

Stirrat A, Gallagher M, Douglas SA, Ohlstein EH, Berry C, Kirk A, Richardson M, and MacLean MR (2001) Potent vasodilator responses to human urotensin-II in human pulmonary and abdominal resistance arteries. *Am J Physiol Heart Circ Physiol* **280:**H925–H928.

Tzanidis A, Hannan RD, Thomas WG, Onan D, Autelitano DJ, See F, Kelly DJ,

Gilbert RE, and Krum H (2003) Direct actions of urotensin II on the heart: implications for cardiac fibrosis and hypertrophy. *Circ Res* **93:**246–253.
Urizar E, Claeysen S, Deupí X, Govaerts C, Costagliola S, Vassart G, and Pardo L (2005) An activation switch in the rhodopsin family of G protein-coupled receptors: the thyrotropin receptor. *J Biol Chem* **280:**17135–17141.
Wise A, Jupe SC, and Rees S (2004) The identification of ligands at orphan G-protein coupled receptors. *Annu Rev Pharmacol Toxicol* **44:**43–66.
Zhai P, Yamamoto M, Galeotti J, Liu J, Masurekar M, Thaisz J, Irie K, Holle E, Yu X, Kupershmidt S, et al. (2005) Cardiac-specific overexpression of AT1 receptor mutant lacking G alpha q/G alpha i coupling causes hypertrophy and bradycardia in transgenic mice. *J Clin Invest* **115:**3045–3056.
Ziltener P, Mueller C, Haenig B, Scherz MW, and Nayler O (2002) Urotensin II mediates ERK1/2 phosphorylation and proliferation in GPR14-transfected cell lines. *J Recept Signal Transduct Res* **22:**155–168.

**Address correspondence to:** Richard Leduc, Ph.D. Department of Pharmacology, Faculty of Medicine and Health Sciences, Université de Sherbrooke, Sherbrooke, Québec, J1H 5N4, ON, Canada. E-mail: richard.leduc@usherbrooke.ca